

# Decision-support tools for diagnosing and selecting the optimal method of repairing buildings

Zbigniew WALCZAK<sup>1</sup>, Barbara KSIT<sup>2</sup> and Anna Szymczak-Graczyk<sup>1\*</sup>

<sup>1</sup> Department of Construction and Geoengineering, Faculty of Environmental and Mechanical Engineering, Poznan University of Life Sciences, Piątkowska 94E, 60-649 Poznań, Poland

<sup>2</sup> Institute of Building Engineering, Faculty of Civil and Transport Engineering, Poznan University of Technology, Piotrowo 5, 60-965 Poznań, Poland

**Abstract.** This study introduces an innovative algorithm that leverages terrestrial laser scanning (TLS) and the fuzzy analytic hierarchy process (FAHP) for the optimization of building repair methodologies. Focusing on multi-criteria decision-making (MCDM), it showcases a methodology for evaluating and selecting the most effective repair strategy for building elements, balancing various conflicting criteria. The research applies TLS for rapid and accurate geometric data acquisition of engineering structures, demonstrating its utility in structural diagnostics and technical condition assessment. A case study on a single-family residential building, experiencing floor deformation in a principal ground-floor room, illustrates the practical application. Maximum deflection and floor deflection distribution were measured using TLS. Utilizing FAHP for analysis, the decision model identifies the most advantageous repair method from a building user's perspective. This approach not only provides a systematic framework for selecting optimal repair solutions but also highlights the potential of integrating advanced scanning technologies and decision-support methods in the field of building materials and structural engineering.

**Keywords:** plate deflection; floor plate repair; terrestrial laser scanning; fuzzy AHP method (FAHP).

## 1. INTRODUCTION

Economic growth, an increase in the wealth of societies as well as rising global population result in an increased demand for constructing various engineering structures. This applies to buildings intended for living, but also to factories, warehouses, and other accompanying infrastructure facilities. During construction work, defects may occur due to human error, unconscious actions, or improperly used materials. Also, during the operation of facilities, there are damages caused by improper use, excessive loads, or violent weather phenomena [1]. Soil deforms under the action of loads, and the resultant deformations depend on their types and values as well as the properties of the soil. The prediction of soil mass deformation is an important issue to be considered in the design of structures. Small deformations of the substrate do not cause even minimal cracks in buildings, while large ones, mostly irregular, usually end in serious damage. Substrate irregularities necessarily require repairs, since leaving them, in extreme cases, may lead to construction disasters [2]. The need for repairs, reinforcements, and modernization generates additional costs that must be borne by users or owners, stimulating the remarkably dynamic development of the branch of the computer-aided construction process. In this case, it focuses on continuous monitoring of structure operation and warnings in the event of exceeding the load capacity and use limits.

One of the methods of obtaining information about buildings is terrestrial laser scanning (TLS), which enables quick measurements of engineering structures. It finds application in the inventory of engineering structures and the development of BIM models, in particular HBIM historical objects, for which the existing plans are incomplete or do not exist. It can also be used to assess the technical condition of structures, e.g. Nowak *et al.* [3] used TLS to assess the technical condition of the Historic Building in Karlino. Szymczak-Graczyk *et al.* [4] used TLS to determine the deflection of the ceiling under the Column Hall of the historic Palace. Such an inventory, if conducted cyclically, at intervals of several months or years, allows for assessing harmful structural changes and their pace. For example, Berberan *et al.* [5] used TLS to monitor the deformation of the dam. Similarly, Gordon *et al.* [6] successfully used TLS for surface deformation measurement. They indicated that TLS could measure vertical deflection with six to 12 times better accuracy than single-point accuracy. It also facilitates quick estimation of the consequences of possible disasters i.e. earthquakes, estimation of the volume of earth masses, and condition of excavation walls [7], particularly when the area is large and there is the risk of trespassing. Also, it is used to estimate and monitor the above-ground biomass (AGB) of trees and to assess the health condition of forest stands. It can be applied in event, accident, or crime scene analysis. Besides, scanning is used to develop visualizations or online tours.

Terrestrial laser scanners can be divided into impulse time-of-flight (ToF) and phase-shift (PS) scanners. In both, objects are illuminated with a beam of light (laser); however, in ToF scanners with pulses, and PS scanners with a continuous beam.

\*e-mail: [anna.szymczak-graczyk@up.poznan.pl](mailto:anna.szymczak-graczyk@up.poznan.pl)

Manuscript submitted 2024-04-11, revised 2024-05-27, initially accepted for publication 2024-08-02, published in November 2024.

Pulse scanners measure the time needed for the beam emitted from the scanner to travel to the measured object and back. The distance can be determined using the equation:

$$L = \frac{c \cdot \Delta t}{2},$$

where  $c$  – light speed [m/s],  $\Delta t$  – scanner beam passage time to the object and back [s].

Phase scanners emit a modulated continuous beam, and the phase shift of the beam reflected from the object is registered in relation to the beam emitted by the scanner. The distance of the object from the scanner can be calculated using the equation:

$$L = \frac{1}{2}N\lambda + \lambda \frac{\Delta\varphi}{2\pi},$$

where  $\lambda = c/f$  – wavelength [m],  $f$  – frequency [Hz],  $\Delta\varphi$  – phase shift [rad],  $N$  – a multiple of the number of full wavelengths.

The beam is deflected vertically ( $\beta$ ) and horizontally ( $\alpha$ ) by the system of rotating mirrors, the angles of mirror deflections are precisely measured during the operation of the scanner. This facilitates the precise determination of the coordinates of measurement points in a 3D coordinate system. The measured distance ( $L$ ) to the  $i$ -th measuring point and the vertical ( $A$ ) and horizontal ( $B$ ) mirror deflection angles facilitate the determination of the position of the measuring point in the 3D coordinate system in real time using the equation:

$$X_i = L \cos \beta \cos \alpha,$$

$$Y_i = L \cos \beta \sin \alpha,$$

$$Z_i = L \sin \beta.$$

Scanners make very dense, quasi-continuous measurements with a speed of approx. a million points per second (PS scanners), enabling precise geometry mapping from the object. In addition, TLS scanning allows for making geometric measurements of objects in hard-to-reach places, the only condition is the visibility of the scanned surface of a given element, and no obstacles obscuring its surface. For places that are difficult to reach for the light beam, for example, high roofs, it is possible to combine laser scanning with photogrammetric techniques or even with classical measurements as proposed by e.g. Gleń *et al.* [8]. Hayakawa *et al.* [9] used TLS and UAV for volume measurement of coastal bedrock erosion. The use of TLS increased the alignment accuracy of various time-series data sets acquired from UAV-SfM to the scale of a few centimeters. Mohammadi *et al.* [10] in creating a digital twin of Australian heritage bridge used UAV photogrammetry and TLS. The use of TLS significantly improved the accuracy of the model and the density of the point cloud. Son *et al.* [11] used UAV and TLS to measure the volume of a landfill. They indicate that the combination of UAV and TLS can be a rational solution for analyzing large sites. Zang *et al.* [12] also propose combining UAV and TLS as a method to detect deformations for hilly areas with limited GCPs.

The use of fast and highly accurate measurement methods such as laser scanning facilitates diagnostics, monitoring, and repairs. It is also convenient for owners or users because there

is no need to use invasive diagnostics at the stage of locating the damage. The use of laser scanning can be classified as a non-destructive diagnostic method. After diagnosing the damage, the next step is to decide how to repair it. The average owner or user would like to make this decision on their own, basing it on information obtained from various sources, i.e., literature, press, and television, or information heard from other people, which is not always advisable.

Selecting the optimal solution to a decision problem requires using multi-criteria decision support methods, MCDM (multi-criteria decision making). These methods allow the comparison of decision variants and the selection of the optimal solution based even on conflicting criteria. The undoubted advantage of the MCDA methods is the ease of solving problems described by various measures. They facilitate the assessment of individual factors, both qualitative and quantitative. They also encourage interested parties, i.e. different communities, to take part in the decision-making process. However, the disadvantages of MCDA methods are related to the risk of subjectivity in assigning weights and priorities to individual criteria by experts in the process of developing a decision-making model. This entails the consequences of obtaining different solutions by different people, depending on their preferences and their priorities as well as the assigned weights of individual criteria. Another drawback of MCDA methodology is the fact that it is a time-consuming process due to the great possibilities for public involvement, particularly at the stage of criteria development, implementation, and data collection.

One of the most popular decision support methods is the AHP – analytic hierarchy process by Saaty [13], commonly applied to numerous engineering problems related to optimization and decision-making. An extensive literature review of the application of AHP in construction management is given, for example, by Darko *et al.* [14]. It can be used in construction, starting from the sustainable selection of materials [15], through construction [16] operation optimization [17], logistics and supplier selection [18], to choosing how to adapt historic buildings and how best to reuse them [19].

In AHP analysis, several decision criteria and sometimes sub-criteria are assigned to a decision problem. Then, a preference matrix of the individual criteria is developed, which represents the importance of each criterion according to the experts in the context of the analyzed decision-making problem. Individual options are assigned ratings within the previously defined criteria. The ratings are assigned by experts or groups of experts, and some of the ratings, especially those that are not quantitative, are assigned subjectively. As a result, some of the ratings may be inaccurate. An increasingly popular alternative to the classical AHP method is the use of fuzzy numbers and the fuzzy AHP (FAHP) method. Demirel *et al.* [20] presented four different approaches to FAHP. An extensive review of the literature published since 2008 in which fuzzy AHP was applied to industrial decision-making problems can be found in Liu *et al.* [21]. Fuzzy numbers allow the uncertainty of the decision-maker to be taken into account and are used to represent human judgments more realistically. Many approaches to fuzzification of AHP methods can be found in the literature [21], depending

on the fuzzification functions used. The most commonly used fuzzification functions are triangular [22], but trapezoidal [23] or spherical [24] functions are also used.

The analysis of the decision problem should also be supplemented by a sensitivity analysis of the model [25]. Sensitivity analysis facilitates the estimation of the uncertainty of the decision model and the impact of the subjectivity of the estimation of the mutual importance of individual criteria [26]. It also provides information about possible changes in the rankings of the alternatives depending on changes in the parameters of the decision model under analysis. Furthermore, it facilitates the estimation of the method stability. In the case of the AHP and FAHP methods, sensitivity analysis is most often performed by modifying the criteria weights in a systematic manner or, in a probabilistic approach, randomly, such as using the Monte Carlo method [27]. Alternatively, the fuzzification factor ( $\Delta$ ) is modified when constructing triangular fuzzy numbers (TFNs). Typically, the initial value of the factor is taken as  $\Delta = 1$ .

The paper aims to present the methodology and the algorithm of proceeding in selecting the method for repairing a deformed building element. The authors propose repair methods used for eliminating deformation caused by soil moisture and irregularities in construction works. They put forward fuzzy AHP as a method of supporting the decision-making process. The method is an extension of classic AHP, in which the uncertainties of selection and estimation of the preference matrix by the decision maker are minimized to some extent by using fuzzy sets. A set of criteria divided into main criteria and sub-criteria is proposed to facilitate the development of a new decision-making model. Naturally, this set can be extended, if necessary, with new main criteria or further sub-criteria. As a result, the methodology can be successfully used for analyzing and decision-making in other situations requiring the selection of the best option for the modernization or repair of buildings. The case study included a deformed floor in a single-family residential building. The idea of the paper is to support the owner or user in the decision-making process regarding construction repair.

The algorithm presented in the article is an innovative solution to the course of action in the case of repairing damages in a building, which is based both on scientific measuring methods and engineering intuition. The hierarchical decision-making model developed by the authors has an applied character and its main advantage is the possibility to adapt it to objects with different surfaces and further use of its capabilities to select the optimal way of repairing other damages in the object.

## 2. MATERIALS AND METHODS

The implementation of decision-making models requires the use of the most complete and reliable input data sets possible, based on objective quantitative and qualitative analyses. For the problem under consideration, data sets concerned both the existing condition of the floor and data on the proposed alternative repair methods. To facilitate the development of the model and the preference matrix for individual criteria, the authors used a division into three main criteria and nine sub-criteria (Table 1). The

economic criterion is objective, quantitative, and relatively easy to determine for individual variants. The technical criteria are quantitative and objective. Both the assessment of repair complexity and the assessment of technology used are qualitative, while the execution time and warranty period are quantitative. The environmental criteria are qualitative.

**Table 1**  
Main criteria and sub-criteria adopted for fuzzy AHP

Criteria	Economic	Execution costs Indirect costs
	Technical	Complexity/difficulty of repair Technology availability/maturity Impact of the change on the object Execution time
	Environmental	Necessity for waste disposal Safety of works Environmental nuisance

The further part of the paper discusses in detail damage assessment procedures as well as conducted geotechnical tests and deformation analysis, which were the basis for proposing alternative methods to repair the floor. The methodology of selecting the most advantageous variant using the FHP method was also discussed thoroughly.

### 2.1. Description of the research object

The case study object presented in the paper is a single-family semi-detached house built in 2007. It is a two-storey building without a basement, with a steep roof, and an area of approx. 100 m<sup>2</sup>. The floor in the largest room located on the ground floor of the building deformed. The deformation was distinctly felt during the use of the building and clearly visible at on-site verification. To collect necessary data, i.e. make an inventory of the layers under wood panels covering the entire room, a test sample was collected (Fig. 1). Figure 1 shows the successive layers of



**Fig. 1.** Test sample with visible successive layers of the floor

the floor, i.e. starting from the top: panels (1 cm thick), yellow foil, cement screed (5 cm thick), polystyrene thermal insulation (8 cm thick), black foil and concrete base (thickness 8 cm).

## 2.2. Geotechnical measurements

In order to investigate the causes of subsidence of the floor in the building, geotechnical tests were performed. Four test holes were drilled from 1.5 to 4.0 m below ground level, a total of 8.0 m (Fig. 2), and 2 dynamic soundings were made from 1.9 to 2.0 m below ground level.



Fig. 2. Location of geotechnical test holes

Geotechnical tests of the 1.5-metre-deep hole in the room (Fig. 2) where the floor was deformed showed that the substrate under the floor consisted of:

- Panels (1 cm thick), yellow foil, cement screed (5 cm thick), polystyrene thermal insulation (8 cm thick), black foil and concrete base (8 cm thick) – 20 cm in total (Fig. 1);
- Uncontrolled bank, with a predominance of fine sand – 60 cm in total, in a loose state, moist on the verge of wet;
- Uncontrolled bank, with a predominance of fine sand and sandy clay, 30 cm in total, in a soft-plastic or plastic state, moist on the verge of wet;
- Brown-grey sandy clay interbedded with fine sand, filling the test hole to the bottom, in a soft-plastic or plastic state, moist on the verge of wet.

The depth of the groundwater table was measured as 80 cm below the level of the top layer of the floor.

## 2.3. TLS measurement

To estimate the deflection and the spatial deformation map of the floor in the room, the floor was scanned with the Faro Focus S70 laser scanner. Scanning was performed in three locations (Fig. 3), the set scanning resolution for each measurement station was  $20714 \times 8534$  points, and the scanning time for a single measurement stand was approx. 15 minutes. To facilitate the subsequent connection of the clouds of points, reference spheres were used (Fig. 4).

The clouds of points were processed in Faro Scene. The clouds from individual stands were combined into one cloud of points, the cloud was filtered by rejecting noise and unnecessary points and then optimized and aligned using the cloud2cloud method.

Then, in the Faro Scene, the scene was cropped so that only the floor remained (Fig. 4) and the final cloud of points was generated, which was then exported to the \*.las format for further

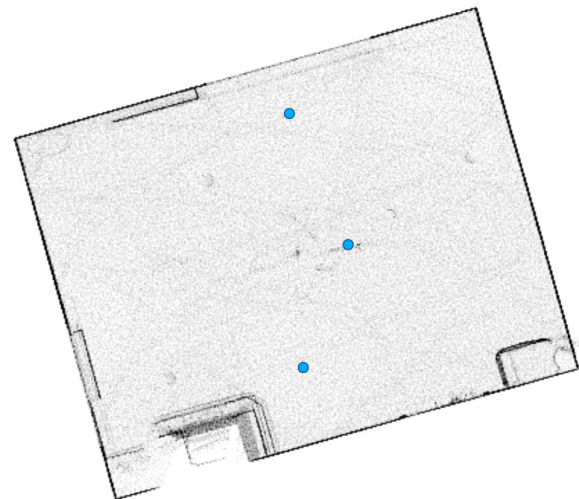


Fig. 3. Location of scanning stands

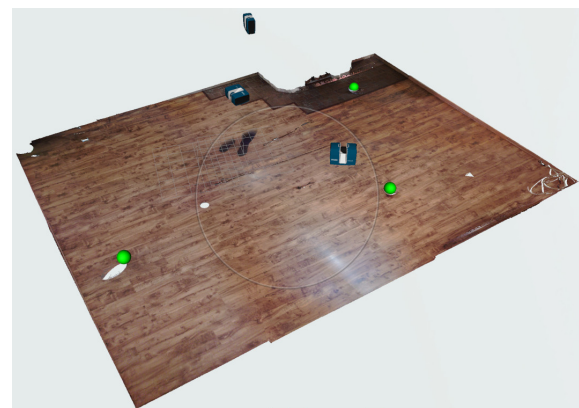


Fig. 4. Developed cloud of points of the analyzed floor

processing in CloudCompare. The final exported cloud subject to processing in CloudCompare consisted of approx. 57 million points. CloudCompare introduced a reference plane in such a way that it was adjacent to the edge of the floor so that the distances between the plane and the point cloud at the edge of the floor were zero. Subsequently, in relation to the reference plane, the distances between the plane and the scanned floor were determined and the floor deformation map was developed.

## 2.4. Assumptions for fuzzy AHP

The construction of the FAHP model involved the division of the decision problem into nine individual criteria (Table 2), which were grouped into three main criteria: economic ( $G_1$ ), technical ( $G_2$ ), and environmental ( $G_3$ ). This created a multi-level hierarchical structure of the problem (Fig. 5). Organizing the problem structure in this way facilitated the development of a preference matrix for each criterion. Table 3 summarizes the criteria adopted and the rating scale use.

Pairwise comparison matrices were constructed for all criteria and sub-criteria using Saaty's nine-point scale [28] (Table 3). The pairwise comparison matrix of the FAHP method was constructed identically as for the classical AHP method

## Decision-support tools for diagnosing and selecting the optimal method of repairing buildings

**Table 2**  
Summary of criteria and adopted rating scales

Criterion identifier and characteristic	Criterion	Rating scale	Explanation of the rating scale
<b>G<sub>1</sub> – Economic</b>			
K <sub>1</sub> destimulant	execution costs	1–3	1 < 10 000 € 2 10 000–15 000 € 3 > 15 000 €
K <sub>2</sub> destimulant	indirect costs	1–2	1 – No additional costs expected 2 – Low probability of additional costs 3 – High probability of additional costs
<b>G<sub>2</sub> – Technical</b>			
K <sub>3</sub> destimulant	complexity/difficulty of repair	1–3	1 – relatively low complexity of repair work 2 – medium complexity of repair work, no highly specialised equipment required 3 – high complexity of repair works, highly specialised equipment required
K <sub>4</sub> destimulant	technology availability/maturity	1–3	1 – technology well known, frequently used 2 – technology relatively new, already proven 3 – new technology, poorly proven
K <sub>5</sub> destimulant	impact of the change on the object	1–4	1 – none 2 – minor adaptation required 3 – major modifications required 4 – very large modifications required
K <sub>6</sub> destimulant	execution time	days	
<b>G<sub>3</sub> – Environmental</b>			
K <sub>7</sub> destimulant	necessity for waste disposal	1–3	1 – no necessity for waste disposal during and after repair 2 – necessity for disposal of materials amassed during the renovation (earth masses, concrete, etc.) 3 – necessity for disposal of harmful and/or dangerous materials
K <sub>8</sub> destimulant	safety of works	1–3	1 – low risk of failure or accident 2 – medium risk of failure or accident 3 – high risk of failure or accident
K <sub>9</sub> destimulant	environmental nuisance	1–3	1 – none 2 – small nuisance, periodic traffic difficulties/none or only periodically/noise 3 – high nuisance

**Table 3**  
Relative Saaty's rating scale [28]

Intensity of importance	Definition	Explanation
1	Equal importance	Two elements contribute equally to the objective
3	Moderate importance	Experience and judgment slightly favour one element over another
5	Strong importance	Experience and judgment strongly favour one element over another
7	Very strong importance	One element is favoured very strongly over another, its dominance is demonstrated in practice
9	Extreme importance	The evidence favouring one element over another is of the highest possible order of affirmation
2, 4, 6, 8 can be used to express intermediate values		

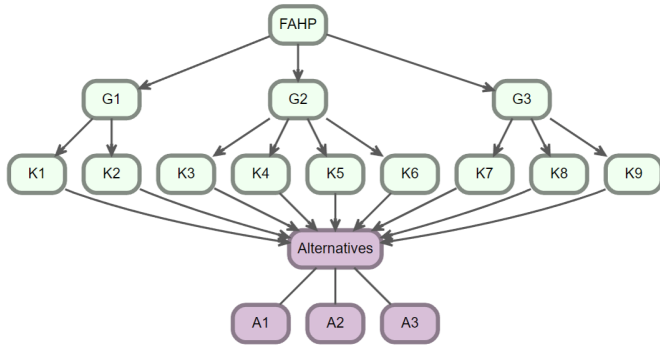


Fig. 5. Hierarchical decision tree of the analysed problem

and then completed by adding fuzzy numbers  $\tilde{c} = (c_1, c_2, c_3)$  as follows [29]:

$$\mu_{\tilde{c}}(x) = \begin{cases} \frac{x - c_1}{c_2 - c_1}, & c_1 < x < c_2 \\ 1, & x = c_2, \\ \frac{c_3 - x}{c_3 - c_2}, & c_2 < x < c_3, \\ 0, & \text{otherwise,} \end{cases} \quad (1)$$

where  $c_1, c_2$ , and  $c_3$  are called lower  $c_1$ , middle  $c_2$ , and upper  $c_3$  significant values, with the middle values equal to the values of the pairwise comparison matrix of the usual AHP method. The lower and upper values were generated using the fuzzification factor  $\Delta = 1$  according to Table 4 [30]. Three matrices were constructed for the sub-criteria, and one for the main criteria,

which consisted of fuzzy numbers vectors:

$$\tilde{B}_k = (\tilde{b}_{ij})_{n \times n} \times \begin{bmatrix} (1, 1, 1) & (l_{12}, m_{12}, u_{12}) & \cdots & (l_{1n}, m_{1n}, u_{1n}) \\ \left(\frac{1}{l_{12}}, \frac{1}{m_{12}}, \frac{1}{u_{12}}\right) & (1, 1, 1) & \cdots & (l_{2n}, m_{2n}, u_{2n}) \\ \vdots & \vdots & \ddots & \vdots \\ \left(\frac{1}{l_{1n}}, \frac{1}{m_{1n}}, \frac{1}{u_{1n}}\right) & \left(\frac{1}{l_{2n}}, \frac{1}{m_{2n}}, \frac{1}{u_{2n}}\right) & \cdots & 1, 1 \end{bmatrix} \quad (2)$$

where  $l_{ij}, m_{ij}$ , and  $u_{ij}$  are lower, middle, and upper values of triangular fuzzy numbers, denoting the dominance of  $i$ -th over  $j$ -th.

The preliminary pairwise comparison matrices from the AHP method were evaluated in terms of quality before fuzzification with the use of the consistency ratio, which also corresponds to checking the fuzzy matrices for consistency only for their medians  $\text{def}(\tilde{c}) = c_2$ :

$$CR = \frac{CI}{RI}, \quad (3)$$

where

$$CI = \frac{\lambda_{\max} - n}{n - 1},$$

$\lambda_{\max}$  – maximum eigenvalue of comparison matrices (maximum eigenvalue),  $n$  – size of comparison matrices ( $n \leq 15$ ),  $RI$  – random index which is obtained by averaging the  $CI$  of a randomly generated reciprocal matrix [31].

CR values for individual matrices should not exceed the threshold of 0.10, otherwise, the pairwise comparison matrix should be re-analyzed.

Table 4

Fuzzy numbers used for making pairwise comparisons [30]

Relative importance	Fuzzy scale	Definition <sup>a</sup>	Explanation
1	(1, 1, 1)	Equal importance	Two activities contribute equally to the objective
3	(3 - Δ, 3, 3 + Δ)	Weak importance	Experience and judgement slightly favour one activity over another
5	(5 - Δ, 5, 5 + Δ)	Essential or strong importance	Experience and judgement strongly favour one activity over another
7	(7 - Δ, 7, 7 + Δ)	Demonstrated importance	One activity is strongly favoured and demonstrated in practice
9	(8, 9, 9)	Extreme importance	The evidence favouring one activity over another is of the highest possible order of affirmation
2, 4, 6, 8	(x - Δ, x, x + Δ)	Intermediate values between two adjacent judgements	When compromise is needed
1/x	(1/(x + Δ), 1/x, 1/(x - Δ))		
1/9	(1/9, 1/9, 1/8)		

<sup>a</sup> Minimum, most likely, and maximum values

<sup>b</sup> Δ is a fuzzification factor

Finally, it is necessary to perform defuzzification of triangular fuzzy numbers. This process can be carried out in several ways, including taking the average value of the three numbers or a weighted average. This article uses the centroid index method, which was developed by Yager and Yager [32]:

$$\text{def}(\tilde{c}) = \frac{(c_2 - c_1) \left( c_1 + \frac{2}{3}(c_2 - c_1) \right) + (c_3 - c_2) \left( c_2 + \frac{1}{3}(c_3 - c_2) \right)}{(c_2 - c_1) + (c_3 - c_2)}. \quad (4)$$

The weights  $\tilde{w}_i = (w_{i1}, w_{i2}, w_{i3})$  of fuzzy comparison matrix, for each obtained matrix, were calculated by the approach described by Enea and Piazza [33], and Krejčí *et al.* [29] by normalizing the geometric means of the rows of the pairwise comparison matrix (see equations (5)–(7)), where  $p$  is the number of  $\tilde{b}_{ij}$  objects on one level of the hierarchy.

$$w_{i1} = \min \left\{ \frac{\sqrt[p]{\prod_{j=1}^n b_{ij}}}{\sum_{k=1}^p \sqrt[p]{\prod_{j=1}^n b_{kj}}}; b_{rs} \in [b_{rs1}, b_{rs3}], \right. \\ \left. r, s = 1, \dots, p, r < s, b_{sr} = \frac{1}{b_{rs}}, r, s = 1, \dots, p, \right. \\ \left. r < s, b_{rr} = 1, r = 1, \dots, p \right\}, \quad (5)$$

$$w_{i2} = \frac{\sqrt[p]{\prod_{j=1}^n b_{ij2}}}{\sum_{k=1}^p \sqrt[p]{\prod_{j=1}^n b_{kj2}}}, \quad (6)$$

$$w_{i3} = \max \left\{ \frac{\sqrt[p]{\prod_{j=1}^n b_{ij}}}{\sum_{k=1}^p \sqrt[p]{\prod_{j=1}^n b_{kj}}}; b_{rs} \in [b_{rs1}, b_{rs3}], \right. \\ \left. r, s = 1, \dots, p, r < s, b_{sr} = \frac{1}{b_{rs}}, r, s = 1, \dots, p, \right. \\ \left. r < s, b_{rr} = 1, r = 1, \dots, p \right\}, \quad (7)$$

A total of four local weight vectors  $\tilde{w}_i = (w_{i1}, w_{i2}, w_{i3})$  were obtained,  $i = 1; 2; 3; 4$ , accordingly for the comparison matrix

of criteria groups  $\tilde{w}_G$  (for  $G_1$ – $G_3$ ) and for individual sub-criteria  $\tilde{w}_{K_i}$ , ( $K_1$ – $K_9$  according to groups – Table 2). The sum of the middle values of weights  $w_{i2}$ , for each of the four local weight vectors, was equal to 1, which is the basic axiom of the AHP method. The difference between the sum of minimum values and maximum values represents a range of uncertainty or fuzziness in the computed weight and can be viewed both as belief and plausibility. The final weight  $\tilde{u}_k = (u_{k1}, u_{k2}, u_{k3})$  for  $k$ -th criterion was designated as:

$$u_{k1} = w_{k1} \cdot w_{G1}; \text{ where } w_{k1} \in G_k, \quad (8)$$

$$u_{k2} = w_{k2} \cdot w_{G2}; \text{ where } w_{k2} \in G_k, \quad (9)$$

$$u_{k3} = w_{k3} \cdot w_{G3}; \text{ where } w_{k3} \in G_k. \quad (10)$$

Then, the obtained weight vectors were defuzzified using the centroidal method (4) proposed by Yager and Yager [32].

The final fuzzy AHP score  $\tilde{F}_{A_i} = (F_{A_i1}, F_{A_i2}, F_{A_i3})$ ,  $i = 1, \dots, m$ ; where  $m = 3$  represents the number of alternatives under consideration, for each alternative was designated as:

$$F_{A_i} = \sum_{k=1}^n V_{A_{ik}} \cdot u_k^d \text{def}(\tilde{c}) = ??, \quad (11)$$

where  $V_{A_{ik}}$  is the  $k$ -th rating (for  $k$ -th category) for the  $i$ -th alternative  $A_i$ , whereas  $u_k^d$  is analogously the  $k$ -th general weight after defuzzification (for the  $k$ -th category).

The analyses used the fuzzy AHP package for R [34] for determining the pairwise comparison matrix and fuzzy local weights  $\tilde{w}_i$  (equations (5)–(7)).

## 2.5. Sensitivity analysis

To assess the impact of the subjectivity of assessing the mutual importance of each criterion and the stability of the built decision model, a sensitivity analysis was conducted. This analysis was conducted by modifying the weights for the main criteria  $G_1$ – $G_3$ , which, of course, translated into the final vector of main weights  $\tilde{u}_k$ . A total of 50 vectors of  $G_1^i$ – $G_3^i$  weights were randomly generated, and for each iteration, the normalized final weights were determined by taking into account all criteria  $K_1$ – $K_9$ . Numerical simulations were conducted on the generated weight matrix to identify the optimal solution using the FAHP method. In this process, 50 rankings were obtained.

## 2.6. Description of repair methods

There are many specialistic methods of repairing damaged floors that collapsed in the ground, these methods focus on the improvement of mechanical parameters of low-bearing soils [35]. The variety of solutions that improve the strength parameters of soil medium results from the type of substrate and the characteristics of the foundations of individual buildings. In the analyzed case, after conducting geotechnical tests using a dynamic probe, which showed poorly compacted soils and voids at a depth of 1 m, three methods of floor repair were selected.

The first method called  $A_1$  for further analysis, involves the demolition of all layers of the floor. An additional difficulty here is the need to take all the furniture out of the room. In the

analyzed case, the room features a fireplace – its structure must be dismantled together with any installations that are routed in the layers of the floor. According to the geotechnical report, in the analyzed building, the substrate must be replaced to the depth of 1 m, the assumed works provide for the installation of a protecting system against groundwater, which is located at a depth of 80 cm. Materials from demolition must be recycled. Both the soil and construction materials, such as polystyrene or waterproofing protection, including roofing felt, are materials that are hazardous to the environment and human health. A1 method is a technology that improves the strength parameters of soil by its compacting or vibrating. Although the method results in soil compaction, it can lead to significant structural damage of the object [36]. Restoring the layers of the floor is also associated with repainting the walls inside the room. The method is time-consuming and requires adequate storage facilities for building materials needed for repair. It is one of the oldest methods of soil strengthening since the first applications of compacting non-cohesive layers were used as long ago as in ancient Egypt [36].

Another method, designated in the paper as A<sub>2</sub>, is a technology using cement grout injection. It is one of static, vibro-compaction methods (Soilfrac). The technology requires precise dosing of pumped volumes of injection grout, working pressure, and to start with – the right selection of compaction grout composition. The injection grout must be of high viscosity and have high solids content. It usually consists of cement, slag, fly ash, filling material (i.e. rock powders), pre-hydrated bentonite, and other additives (i.e. setting accelerants) as well as water [35]. The technology consists of installing injection pipes in the soil (Fracs), into which the hardening grout is pumped. Vibro-compaction injection is performed multiple times, in stages, at least in three phases to obtain the appropriate compaction of soil [36]. The technology requires the use of specialized equipment and qualified employees. Soil compaction works should also be monitored and supervised. The floor layer must be dismantled, however, there is no need to remove the concrete layer or the existing fireplace. The injection grout is introduced into holes arranged as a grid with a side spacing of 0.33 to 1 m, through double packers. The method is considered time-consuming, the shortest time to obtain soil strength parameters is seven days from the moment of grout injection. It is also classified as dirty work, as drilling pits are required. After the pumping is completed, the injection pipe is thoroughly cleaned, which determines the repetition of the injection. The technology developed in the 1970s, the first attempts to pump a thick cement mortar into the ground to compact loosened soil zones took place in the 1950s in California [37].

The third method of repair is geopolymer injection, for further analysis called A<sub>3</sub>. It is a fast-expanding, high- or low-pressure method classified as static. For this technology, the most used materials are flexible or hard-elastic, foamable or non-foaming, and one- and two-component injection materials based on resins. The technology requires trained personnel and constant monitoring of the structure operation during the process of introducing the material into the soil medium [38]. It does not require the removal of objects from rooms; however, it can damage sewer

pipes and plug drains. The grout is injected into holes arranged as a grid on the floor with a side spacing of 1 to 1.5 m, the thickness of holes can be from 14–20 mm. The material reaches 90% of its final strength within 15 minutes of finishing injection. Such a rapid increase in strength parameters means that the floor can be ready to use again after a very short time [39]. The technology does not require a technological park and heavy construction equipment as appropriate technological equipment fits in a car. Injection works are performed without the need to dismantle floor layers and thus no disposal of building materials is required. The geopolymer injection method has been used for 30 years.

### 3. RESULTS

#### 3.1. Measurements of deformation of the room floor

Measurements of floor deformation distribution were made using TLS laser scanning. TLS measurements were taken at three measurement stations. Three separate point clouds were obtained. Point clouds from three measurement stations were merged in Faro Scene software, resulting in a single dense point cloud. The accuracy of the cloud2cloud point cloud merging was Maximum point error 0.6 mm, Average point error 0.6 mm, and Minimum overlap 85.2%. The accuracy of 0.6 mm refers to the quality of the merging of point clouds and is based on the distances between overlapping point clouds. The values were determined by the Faro Scene software.

The cropped cloud of points was imported into CloudCompare, and a horizontal reference plane was introduced. The cloud and the plane were adjusted so that the plane touched the edges of the cloud of points. Then, the distribution of floor deflections was determined, i.e. the distribution of distances (normal) between the reference plane and the cloud of points (Fig. 6). The location of the plane was assumed arbitrarily. The developed layout is a visualization of the map of the height of the floor face below the assumed comparative level (reference plane).

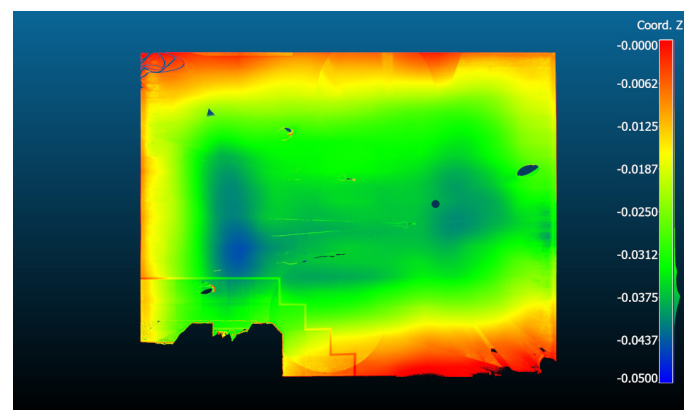


Fig. 6. Distribution of distances between the reference plane and the cloud of points – the map of floor deflections

In addition, Fig. 7 shows the distribution of distances in the form of a histogram. The average difference in the position of



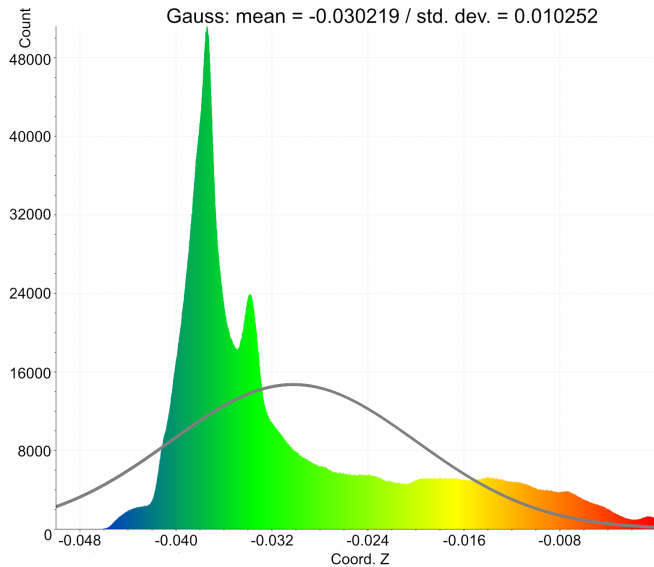


Fig. 7. Histogram of floor plate deflections

points (point cloud – reference plane) was 3.0 cm with a standard deviation of approx. 1 cm.

The maximum recorded deflection of the plate was 4.5 cm and occurred near the fireplace (point 1 in Fig. 8, Table 5)

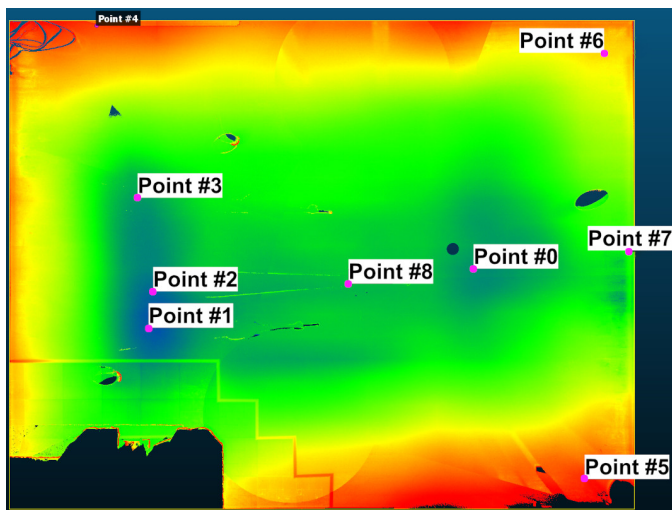


Fig. 8. Location of measuring points

In civil engineering, industrial, and agricultural construction, if no special restrictions for deflections due to special conditions of use are required, the verification of deflections is only necessary for roof and ceiling elements. Thus, there are no requirements with reference to the limit value of deflections of floor plates. However, for illustrative purposes in this paper, it was assumed the limit deflection of  $L/200$  [40], which, taking into account the span of the room, was  $L/200 = 5.4 \text{ m}/200 = 2.7 \text{ cm}$ . By analyzing the deflections provided in Table 5, it can be concluded that plate deflections below 1 cm are only less than 9% of the plate surface, while plate deflections above 2.7 cm [40] are over 57% of the floor surface (Fig. 9). Therefore, it can

Table 5

Measured deflections [m] (designations of points in Fig. 8)

No.	X	Y	Z
0	-1.389	-1.083	-0.040
1	-4.185	-1.593	-0.045
2	-4.143	-1.278	-0.043
3	-4.277	-0.481	-0.039
4	-4.633	0.994	-0.004
5	-0.440	-2.890	-0.001
6	-0.251	0.735	-0.014
7	-0.070	-0.929	-0.031
8	-2.469	-1.214	-0.037

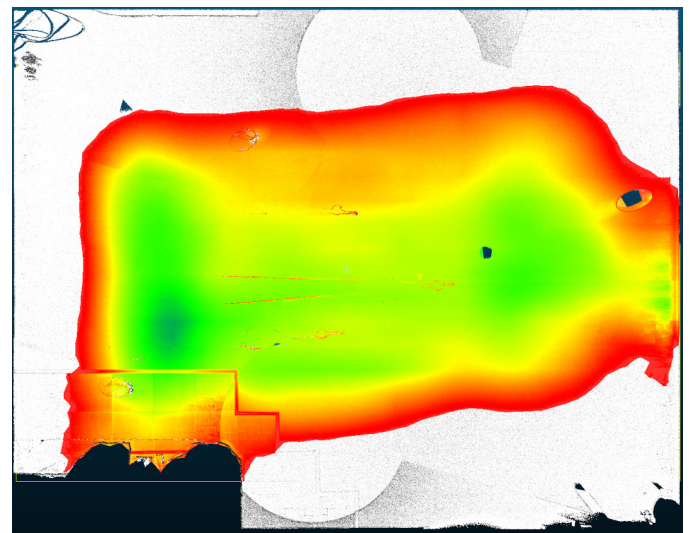


Fig. 9. Area of the floor with more than 2.7 cm deflections

be unequivocally concluded that the values of deflections are unacceptable since they exceed the serviceability limit state.

Figures 10a and 10b show the transverse profiles of the plate in characteristic places, with the greatest deflections.

It can be observed that the face of the floor significantly deviates from the reference plane, with a maximum deflection of approx. 4.5 cm.

### 3.2. FHAP analysis

Three variants of floor repair were proposed:

- Variant 1 (Alternative  $A_1$ ) – demolition of the floor and replacement of the substrate along with appropriate soil compaction;
- Variant 2 (Alternative  $A_2$ ) – cement grout injection;
- Variant 3 (Alternative  $A_3$ ) – geopolymer injection.

The conducted analyses allowed for developing the ratings for individual variants/alternatives in reference to the analysed criteria. The adopted ratings are summarized in Table 6.

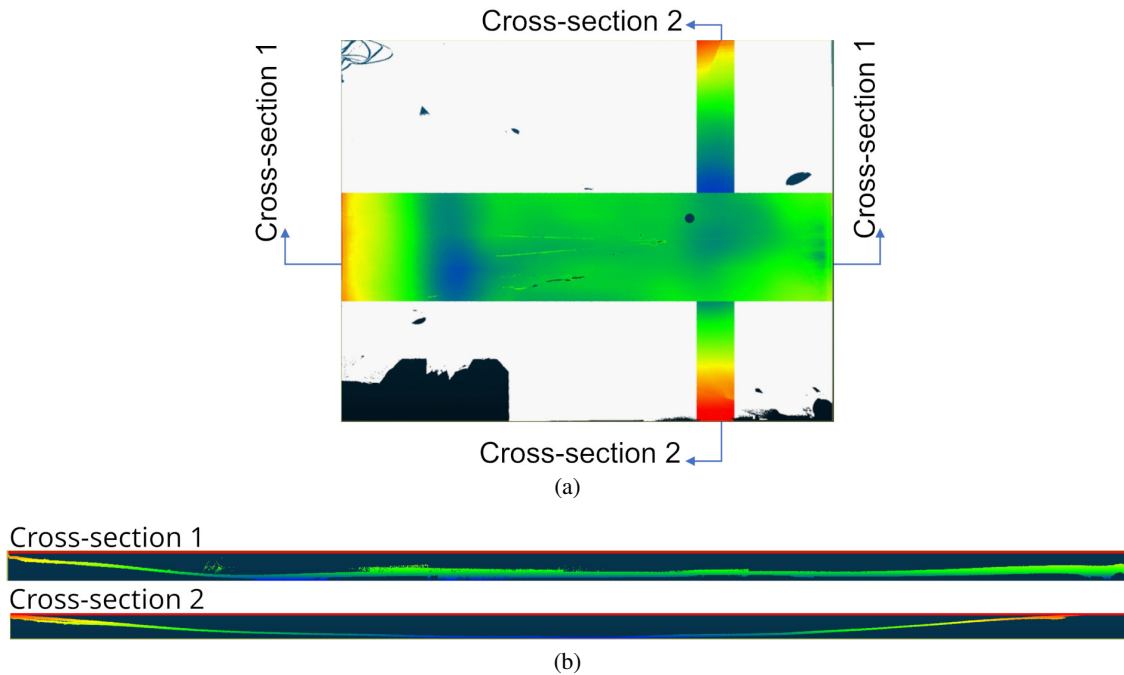


Fig. 10. Location of selected cross-sections (a) and cross-sections of the floor plate (b)

Table 6

Summary of ratings of individual criteria of the considered variants of land development changes

Criterion	Rating scale	s/d*	Variant			
			A <sub>1</sub>	A <sub>2</sub>	A <sub>3</sub>	
G <sub>1</sub> – Economic						
K <sub>1</sub>	execution costs	1–3	d	3	1	1
K <sub>2</sub>	indirect costs	1–3	d	3	1	1
G <sub>2</sub> – Technical						
K <sub>3</sub>	complexity of repair	1–3	d	3	2	1
K <sub>4</sub>	technology availability/maturity	1–3	d	1	2	2
K <sub>5</sub>	impact of the change on the object	1–4	d	4	2	2
K <sub>6</sub>	execution time	days	d	3	2	1
G <sub>3</sub> – Environmental						
K <sub>7</sub>	necessity for waste disposal	1–3	d	3	1	1
K <sub>8</sub>	safety of works	1–3	d	3	2	2
K <sub>9</sub>	environmental nuisance	1–3	d	3	3	1

\* s – stimulant; d – destimulant

As the basis for further considerations, initial pairwise comparison matrices for the classical AHP method were adopted, which were then fuzzified according to Table 4. Four fuzzy pairwise comparison matrices were obtained (Tables 7–10), with the fuzzification factor assumed as  $\Delta = 1$ .

The analyses used the fuzzyAHP package, version 0.9.5 for R for the fuzzification of the pairwise comparison matrix and determination of local weight vectors  $\tilde{w}_i = (w_{i1}, w_{i2}, w_{i3})$ . Local weight vectors for fuzzy numbers were determined using

equations (5)–(7). Global weight vectors  $\tilde{u}_k = (u_{k1}, u_{k2}, u_{k3})$  (Table 11) were determined according to equations (8)–(10).

Then the weights were subjected to the process of defuzzification, in line with formula (4), obtaining the final weight vector (Table 11). The final rating (Table 12) was determined in accordance with equation (11).

The obtained final rating  $A_3 \rightarrow A_2 \rightarrow A_1$  indicates a definite advantage of modern repair methods with a slight difference between geopolymer injections – 43.35 points and cement in-

## Decision-support tools for diagnosing and selecting the optimal method of repairing buildings

**Table 7**Fuzzy pairwise comparison matrix for criteria  $G_1$ – $G_3$ 

	$G_1$	$G_2$	$G_3$
$G_1$	(1; 1; 1)	(4; 5; 6)	(6; 7; 8)
$G_2$	(1/6; 1/5; 1/4)	(1; 1; 1)	(2; 3; 4)
$G_3$	(1/8; 1/7; 1/6)	(1/4; 1/3; 1/2)	(1; 1; 1)

**Table 8**Fuzzy pairwise comparison matrix for criteria  $K_1$ – $K_2$ 

	$K_1$	$K_2$
$K_1$	(1; 1; 1)	(6; 7; 8)
$K_2$	(1/8; 1/7; 1/6)	(1; 1; 1)

**Table 9**Fuzzy pairwise comparison matrix for criteria  $K_3$ – $K_6$ 

	$K_3$	$K_4$	$K_5$	$K_6$
$K_3$	(1; 1; 1)	(1/8; 1/7; 1/6)	(1/6; 1/5; 1/4)	(1/9; 1/9; 1/8)
$K_4$	(6; 7; 8)	(1; 1; 1)	(1/4; 1/3; 1/2)	(1/6; 1/5; 1/4)
$K_5$	(4; 5; 6)	(2; 3; 4)	(1; 1; 1)	(1/3; 1/2; 1)
$K_6$	(8; 9; 9)	(4; 5; 6)	(1; 2; 3)	(1; 1; 1)

**Table 10**Fuzzy pairwise comparison matrix for criteria  $K_7$ – $K_9$ 

	$K_7$	$K_8$	$K_9$
$K_7$	(1; 1; 1)	(1/8; 1/7; 1/6)	(1/3; 1/2; 1)
$K_8$	(6; 7; 8)	(1; 1; 1)	(4; 5; 6)
$K_9$	(1; 2; 3)	(1/6; 1/5; 1/4)	(1; 1; 1)

**Table 11**Fuzzy weights for criteria  $K_1$ – $K_9$ 

	$K_1$	$K_2$	$K_3$	$K_4$	$K_5$	$K_6$	$K_7$	$K_8$	$K_9$
fnMin*	58.43	7.57	0.52	1.68	3.13	6.17	0.47	4.51	0.77
fnModal*	63.93	9.13	0.77	2.69	5.38	10.01	0.76	5.99	1.35
fnMax*	68.38	10.99	1.21	4.45	9.31	14.18	1.44	8.23	2.31
dfnW*	62.80	9.12	0.82	2.90	5.87	9.99	0.88	6.17	1.46

\* fnMin – fuzzy weights for low fuzzy numbers  $u_{k1}$ , fnModal – fuzzy weights for middle fuzzy numbers  $u_{k2}$ , fnMax – fuzzy weights for upper fuzzy numbers  $u_{k3}$ , dfnW – vector of weights used to calculate the final rating of fuzzy AHP

jections – 38.92 points. The traditional approach related to soil replacement scored only 16.82 points. The ranking position was determined particularly by economic criteria ( $G_1$ ), in which cri-

**Table 12**Summary of fuzzy AHP results for individual scenarios  $A_1$ – $A_3$ 

	$A_1$	$A_2$	$A_3$
Repair of the floor	<b>16.82</b>	<b>39.82</b>	<b>43.35</b>
$G_1$	10.27	30.82	30.82
$K_1$	8.97	26.91	26.91
$K_2$	1.30	3.91	3.91
$G_2$	4.59	6.02	8.97
$K_3$	0.15	0.22	0.45
$K_4$	1.45	0.73	0.73
$K_5$	1.17	2.35	2.35
$K_6$	1.82	2.73	5.45
$G_3$	1.96	2.98	3.56
$K_7$	0.13	0.38	0.38
$K_8$	1.54	2.31	2.31
$K_9$	0.29	0.29	0.87

terion  $K_1$  prevailed for alternatives  $A_2$  and  $A_3$ . Alternatives  $A_1$  and  $A_2$  obtained the same number of points for criterion  $K_1$ , much better than alternative  $A_1$ . Criterion  $K_6$  (execution time) was decisive in selecting the final variant of repair  $A_3$ , which scored the highest number of points here. Alternative  $A_1$  turned out to be the least favourable practically in all respects except for category  $K_4$ . Alternative  $A_3$  proved to be the most favourable for criteria  $G_2$  and  $G_3$  and obtained the same score in the category  $G_1$  as alternative  $A_2$ .

**3.3. Sensitivity analysis**

The authors also performed a sensitivity analysis of the model. 50 normalized weight vectors  $\tilde{u}_G$  modifying only the weights of main criteria  $G_1$ – $G_3$  (Fig. 11) were randomly generated. In each iteration, the global weights were obtained by multiplying the local weights of criteria  $K_1^i$ – $K_9^i$ , previously obtained for the pairwise comparison matrix (Tables 8–10) and subjected to the defuzzification process (equation (4)), by the normalized weights of the main criteria  $G_1^i$ – $G_3^i$  according to equations (8)–(10).

The sensitivity analysis shows that the ranking is very stable and practically unchanging. It was in line with the previously obtained results for alternatives  $A_3 \rightarrow A_2 \rightarrow A_1$  for every iteration. Alternative  $A_1$  obtained an average score of 20.11 (median 20.06, SD = 1.4191), alternative  $A_2$  – 36.53 (median 36.57, SD = 1.7498), and alternative  $A_3$  – 43.29 (median 43.29, SD = 0.6303), respectively (Fig. 12).

The most important criteria are economic criteria related to the cost of execution ( $K_1$ ), environmental criteria related to the safety of the work ( $K_8$ ), and technical criteria related to the execution time ( $K_6$ ).

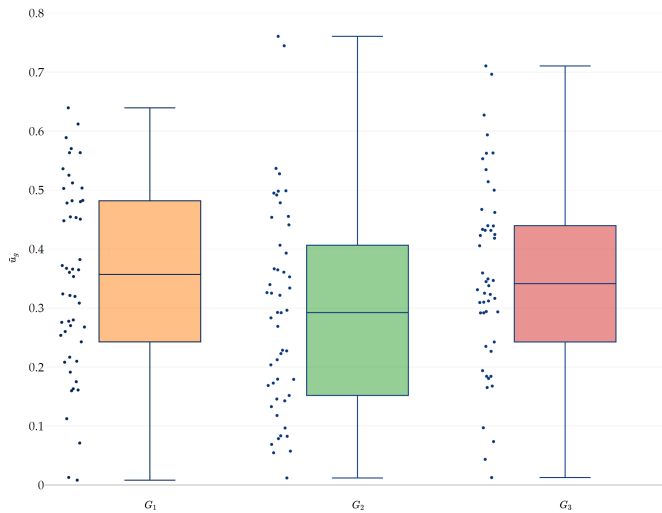


**Fig. 11.** Statistics of generated weights for the group of main criteria  $G_1$ – $G_3$

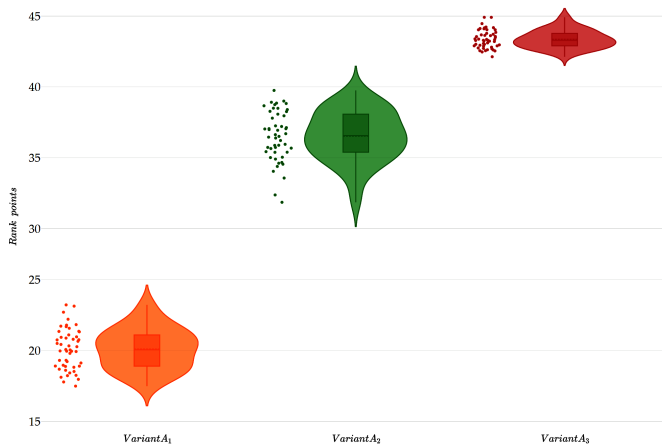


**Fig. 12.** Distribution of points obtained in the rankings of the FAHP method for individual alternatives obtained for 50 iterations of random weight  $\tilde{u}_G$

#### 4. DISCUSSION

The paper presents the usability of modern measurement and diagnostic methods, MCDA methods (FAHP), for diagnosing and selecting the optimal way to repair buildings. As a case study, a single-family house was used, in which the floor was deformed. The study used terrestrial laser scanning to evaluate the deformation and determine the spatial deformation and maximum deflection of the floor. The analysis shows that the deflection above 2.7 cm, which is more than  $L/200$ , is an area of more than 57% of the floor. The maximum deflection is up to 4.5 cm. Repair is required because the deflections exceed the serviceability limit state. Deformations greater than 2.7 cm were observed in the central part of the floor and near the fireplace. The largest deformations were observed in the section of the floor near and in front of the fireplace. This may be related to the additional load on the structure from the fireplace itself. Of course, the additional load on the floor structure is not the main cause of its deformation. Based on the geotechnical

investigation, it can be concluded that the main cause was the inadequate quality of the substructure, which consisted of loose and extremely loose fine sands and sandy loams mixed with humus in a soft-plastic state. In addition, the high variability of the water table and its very high level may have further compromised the consolidation of the substructure. TLS scanning proved to be a very good and accurate tool for estimating the condition of the site. The speed, quantity, and precision of the data acquisition, which represents the geometry of the object, thanks to the high density of the sampling, which is practically continuous and not point by point, makes it possible to use this technique in a wide range of diagnostics of building structures. For example, Szymczak *et al.* [4] used laser scanning to determine the deflections of the ceiling in a historic palace, helping to select the right locations for test holes, which should generally be as few as possible in historic buildings. The given procedure may reduce the need to make test holes that destroy the historic structure of these buildings. The results obtained with the use of a coordinate measuring arm, i.e. a scanner with a measuring head are presented in [41], in which the numerical calculations of a tank with walls of linearly variable thickness were verified. The use of laser scanning to determine the deflections of excavation support plates is shown in [7], where the results obtained from strain gauges were compared with the results from laser scanning. It can be acknowledged that the measurement method using a laser scanner is one of the most advanced, and the results obtained are fully consistent with the ones calculated using numerical methods.

The final ranking of the decision model indicates that in the context of the proposed nine criteria, the optimal variant for floor repair is variant  $A_3$  consisting of geopolymer injection. The method is characterized by the fact that it does not require the removal of objects from the rooms. In the proposed decision model, the main focus was placed on three criteria: cost of repair (criterion  $K_1$ ), environmental criteria related to the safety of the work ( $K_8$ ), and technical criteria related to the execution time ( $K_6$ ). The ranking analysis shows that for the economic criterion  $G_1$ , the  $A_2$  and  $A_3$  variants have the same ranking of 30.82%. Variants  $A_2$  and  $A_3$  also have the same ranking for criterion  $K_8$ . Variants  $A_2$  and  $A_3$  practically have the same placement in each criterion. The exceptions in favor of variant  $A_3$  are criteria  $K_6$  and  $K_9$ , and it was mainly criterion  $K_6$  that decided the optimal variant in this case (between  $A_2$  and  $A_3$ ). The sensitivity analysis also confirmed the stability of the ranking and the greatest influence on the ranking of the criteria  $K_1$ ,  $K_8$ , and  $K_6$ .

The proposed decision model can be used directly (preference matrices and weights of individual criteria) to analyze other cases requiring the selection of the optimal method of modernization or repair. Indeed, the model can be extended with other criteria specific to the problem. The preference matrices and the final vector of weights should then be redefined. In the case of AHP/FAHP, the main source of error or uncertainty that can arise during the construction and analysis of a decision model is the subjectivity of the assignment of preferences/validity to individual criteria by experts. This is true for many decision methods that require experts to indicate their preferences, e.g. by constructing a comparison matrix or by directly indicating

the weights of individual criteria. One of the methods of dealing with uncertainty is the use of fuzzy numbers in the construction of pairwise comparison matrices, as proposed by the authors.

The possibility of applying multi-criteria decision support methods to numerous engineering problems means that testing them beforehand and developing an algorithm for proceeding in a specific case will attract the interest of potential users. The paper presents the procedure for choosing the best location from the point of view of many participants in the decision-making process, considering both social and commercial interests. MCDM methods were successfully used in civil engineering construction for selecting building materials during construction works and at the later stage of use of buildings [15]. A deformed floor in a single-family residential building was used as a case study. In such cases, generally accepted and applied repair methods are considered alternatives to the FAHP method, and their selection is underpinned by the analysis of structural repair issues. Both methods, traditional soil replacement, and grout injection, have been used for years. They are proven and recommended for use to repair damage shown in the work.

## 5. CONCLUSIONS

The idea of the paper was to indicate how to develop a proprietary algorithm for proceeding in selecting the method for repairing building elements. The cited and systematized principles of the FAHP method show its effectiveness for use by owners or users of buildings. A single-family residential building, in which the floor in the largest room on the ground floor was deformed, served as a research example. Based on the measurements, tests, and analyses conducted, the following general conclusions can be drawn:

- Laser scanning is a very effective and proven tool for non-destructive diagnostics of buildings.
- The presented “step-by-step” procedure for the multi-criteria selection method will facilitate the adaptation of the method to other damage cases for which a repair method will be sought.

Detailed conclusions refer to the case study – the deformed floor in question. The deformation of the floor, based on the performed geotechnical tests, was caused by an inadequate quality of the substrate, which consisted of loose and extremely loose fine sands and sandy clay mixed with humus in a soft-plastic state. An additional factor affecting the process of improper consolidation of the prepared substrate was the high and seasonally variable groundwater level, which in the extreme was approx. 20 cm below the floor level. The subsequent formation of voids in the soil structure could lead to the loss of the bearing capacity of the substrate.

From the presented three variants of repair ( $A_1$  – demolition of the floor and replacement of the substrate along with appropriate soil compaction;  $A_2$  – injection of cement grout;  $A_3$  – injection of geopolymers), based on the AHP method, the final rating was obtained. It indicated variant  $A_3$  as the most advantageous, variant  $A_2$  as the second, and variant  $A_1$  as the least beneficial. The difference in points obtained between methods  $A_3$  and  $A_2$  was approx. 4%, whereas it was over 26% between  $A_3$  and  $A_1$ . The position in the ranking was largely determined

by the economic criterion and the time of execution. Variant  $A_1$  turned out to be the least favourable in virtually every criterion considered.

The proposed methodology is a universal solution, independent of the type of building. It can be applied to a building with a small area or a large building, and the evaluation procedure can follow the proposed methodology both to obtain results and to select the most favorable way to repair the damaged structure.

The authors plan to further analyze the feasibility of using TLS and FAGP methods in the evaluation, and diagnosis of engineering structures and construction of a tool to support the decision-making process related to the selection of optimal ways to repair or upgrade the facility. The work will also include analysis of decision-making models in terms of their stability, and the impact of uncertainty in the creation of pairwise comparison matrices on the final rankings.

## REFERENCES

- [1] B. Ksit and A. Szymczak-Graczyk, “Rare weather phenomena and the work of large-format roof coverings,” *Civ. Environ. Eng. Rep.*, vol. 29, no. 3, pp. 123–133, 2019, doi: [doi.org/10.2478/ceer-2019-0029](https://doi.org/10.2478/ceer-2019-0029).
- [2] A. Szymczak-Graczyk, I. Laks, B. Ksit, and M. Ratajczak, “Analysis of the impact of omitted accidental actions and the method of land use on the number of construction disasters (a case study of Poland),” *Sustainability*, vol. 13, no. 2, p. 618, 2021, doi: [10.3390/su13020618](https://doi.org/10.3390/su13020618).
- [3] R. Nowak, R. Orłowicz, and R. Rutkowski, “Use of TLS (LiDAR) for building diagnostics with the example of a historic building in Karlino,” *Buildings*, vol. 10, no. 2, p. 24, 2020, doi: [10.3390/buildings10020024](https://doi.org/10.3390/buildings10020024).
- [4] A. Szymczak-Graczyk, Z. Walczak, B. Ksit, and Z. Szyguła, “Multi-criteria diagnostics of historic buildings with the use of 3D laser scanning (a case study),” *Bull. Pol. Acad. Sci. Tech. Sci.*, vol. 70, no. 2, p. e140373, 2022, doi: [10.24425/bpasts.2022.140373](https://doi.org/10.24425/bpasts.2022.140373).
- [5] A. Berberan, I. Ferreira, E. Portela, S. Oliveira, A. Oliveira, and B. Baptista, “Overview on terrestrial laser scanning as a tool for dam surveillance,” in *6th International Dam Engineering Conference. LNEC, Lisboa*, 2011.
- [6] S.J. Gordon, D. Lichti, M. Stewart, and J. Franke, “Structural deformation measurement using terrestrial laser scanners,” *Proc. 11th FIG Symposium on Deformation Measurements*, Santorini, Greece, 2003.
- [7] M. Kopras, W. Buczkowski, A. Szymczak-Graczyk, Z. Walczak, and S. Gogolik, “Experimental Validation of Deflections of Temporary Excavation Support Plates with the Use of 3D Modelling,” *Materials*, vol. 15, no. 14, p. 14, 2022, doi: [10.3390/ma15144856](https://doi.org/10.3390/ma15144856).
- [8] P. Gleń and K. Krupa, “Comparative analysis of the inventory process using manual measurements and laser scanning,” *Budownictwo i Architektura*, vol. 18, no. 2, pp. 021–030, 2019, doi: [10.35784/bud-arch.552](https://doi.org/10.35784/bud-arch.552).
- [9] Y.S. Hayakawa and H. Obanawa, “Volume Measurement of Coastal Bedrock Erosion Using UAV and TLS,” in *IGARSS 2020-2020 IEEE International Geoscience and Remote Sensing Symposium*, 2020, pp. 5230–5233, doi: [10.1109/IGARSS39084.2020.9323220](https://doi.org/10.1109/IGARSS39084.2020.9323220).
- [10] M. Mohammadi, M. Rashidi, V. Mousavi, A. Karami, Y. Yu, and B. Samali, “Quality evaluation of digital twins generated based

- on UAV photogrammetry and TLS: Bridge case study,” *Remote Sens.*, vol. 13, no. 17, p. 3499, 2021, doi: [10.3390/rs13173499](https://doi.org/10.3390/rs13173499).
- [11] S.W. Son, D.W. Kim, W.G. Sung, and J.J. Yu, “Integrating UAV and TLS approaches for environmental management: A case study of a waste stockpile area,” *Remote Sens.*, vol. 12, no. 10, p. 1615, 2020, doi: [10.3390/rs12101615](https://doi.org/10.3390/rs12101615).
- [12] Y. Zang, B. Yang, J. Li, and H. Guan, “An accurate TLS and UAV image point clouds registration method for deformation detection of chaotic hillside areas,” *Remote Sens.*, vol. 11, no. 6, p. 647, 2019, doi: [10.3390/rs11060647](https://doi.org/10.3390/rs11060647).
- [13] T. L. Saaty, “Decision making with the analytic hierarchy process,” *Int. J. Serv. Sci.*, vol. 1, no. 1, pp. 83–98, 2008, doi: [10.1504/IJSSCI.2008.017590](https://doi.org/10.1504/IJSSCI.2008.017590).
- [14] A. Darko, A.P.C. Chan, E.E. Ameyaw, E.K. Owusu, E. Pärn, and D.J. Edwards, “Review of application of analytic hierarchy process (AHP) in construction,” *Int. J. Constr. Manag.*, vol. 19, no. 5, pp. 436–452, 2019, doi: [10.1080/15623599.2018.1452098](https://doi.org/10.1080/15623599.2018.1452098).
- [15] P.O. Akadiri, P.O. Olomolaiye, and E.A. Chinyio, “Multi-criteria evaluation model for the selection of sustainable materials for building projects,” *Autom. Constr.*, vol. 30, pp. 113–125, 2013, doi: [10.1016/j.autcon.2012.10.004](https://doi.org/10.1016/j.autcon.2012.10.004).
- [16] C.J. Hopfe, G.L. Augenbroe, and J.L. Hensen, “Multi-criteria decision making under uncertainty in building performance assessment,” *Build. Environ.*, vol. 69, pp. 81–90, 2013, doi: [10.1016/j.buildenv.2013.07.019](https://doi.org/10.1016/j.buildenv.2013.07.019).
- [17] D.E. Ighravwe and S.A. Oke, “A multi-criteria decision-making framework for selecting a suitable maintenance strategy for public buildings using sustainability criteria,” *J. Build. Eng.*, vol. 24, p. 100753, 2019, doi: [10.1016/j.jobe.2019.100753](https://doi.org/10.1016/j.jobe.2019.100753).
- [18] C.-H. Chen, “A novel multi-criteria decision-making model for building material supplier selection based on entropy-AHP weighted TOPSIS,” *Entropy*, vol. 22, no. 2, p. 259, 2020, doi: [10.3390/e22020259](https://doi.org/10.3390/e22020259).
- [19] H.-A.A.F. Haroun, A.F. Bakr, and A.E.-S. Hasan, “Multi-criteria decision making for adaptive reuse of heritage buildings: Aziza Fahmy Palace, Alexandria, Egypt,” *Alex. Eng. J.*, vol. 58, no. 2, pp. 467–478, 2019, doi: [10.1016/j.aej.2019.04.003](https://doi.org/10.1016/j.aej.2019.04.003).
- [20] T. Demirel, N.Ç. Demirel, and C. Kahraman, “Fuzzy analytic hierarchy process and its application,” in *Fuzzy multi-criteria decision making*, Springer, 2008, pp. 53–83.
- [21] Y. Liu, C.M. Eckert, and C. Earl, “A review of fuzzy AHP methods for decision-making with subjective judgements,” *Expert Syst. Appl.*, vol. 161, p. 113738, 2020, doi: [10.1016/j.eswa.2020.113738](https://doi.org/10.1016/j.eswa.2020.113738).
- [22] A.N. Patil, “Fuzzy AHP methodology and its sole applications,” *Int. J. Manag. Res. Rev.*, vol. 8, no. 5, pp. 24–32, 2018.
- [23] J.J. Buckley and V.R.R. Uppuluri, “Fuzzy hierarchical analysis,” in *Uncertainty in Risk Assessment, Risk Management, and Decision Making*, Springer, 1987, pp. 389–401.
- [24] F.K. Gündoğdu and C. Kahraman, “A novel spherical fuzzy analytic hierarchy process and its renewable energy application,” *Soft Comput.*, vol. 24, no. 6, pp. 4607–4621, 2020, doi: [10.1007/s00500-019-04222-w](https://doi.org/10.1007/s00500-019-04222-w).
- [25] I. Laks, Z. Walczak, and N. Walczak, “Fuzzy analytical hierarchy process methods in changing the damming level of a small hydropower plant: Case study of Rosko SHP in Poland,” *Water Resour. Ind.*, vol. 29, p. 100204, 2023, doi: [10.1016/j.wri.2023.100204](https://doi.org/10.1016/j.wri.2023.100204).
- [26] B.C. Balusa and A.K. Gorai, “Sensitivity analysis of fuzzy-analytical hierarchical process (FAHP) decision-making model in selection of underground metal mining method,” *J. Sustain. Min.*, vol. 18, no. 1, pp. 8–17, 2019, doi: [10.1016/j.jsm.2018.10.003](https://doi.org/10.1016/j.jsm.2018.10.003).
- [27] L. Serrano-Gomez and J.I. Munoz-Hernandez, “Monte Carlo approach to fuzzy AHP risk analysis in renewable energy construction projects,” *PloS One*, vol. 14, no. 6, p. e0215943, 2019, doi: [10.1371/journal.pone.0215943](https://doi.org/10.1371/journal.pone.0215943).
- [28] T.L. Saaty, “How to make a decision: the analytic hierarchy process,” *Eur. J. Oper. Res.*, vol. 48, no. 1, pp. 9–26, 1990, doi: [10.1016/0377-2217\(90\)90057-I](https://doi.org/10.1016/0377-2217(90)90057-I).
- [29] J. Krejčí, O. Pavlačka, and J. Talašová, “A fuzzy extension of Analytic Hierarchy Process based on the constrained fuzzy arithmetic,” *Fuzzy Optim. Decis. Mak.*, vol. 16, no. 1, pp. 89–110, 2017, doi: [10.1007/s10700-016-9241-0](https://doi.org/10.1007/s10700-016-9241-0).
- [30] S. Tesfamariam and R. Sadiq, “Risk-based environmental decision-making using fuzzy analytic hierarchy process (F-AHP),” *Stoch. Environ. Res. Risk Assess.*, vol. 21, no. 1, pp. 35–50, 2006, doi: [10.1007/s00477-006-0042-9](https://doi.org/10.1007/s00477-006-0042-9).
- [31] R.W. Saaty, “The analytic hierarchy process – what it is and how it is used,” *Math. Model.*, vol. 9, no. 3, pp. 161–176, Jan. 1987, doi: [10.1016/0270-0255\(87\)90473-8](https://doi.org/10.1016/0270-0255(87)90473-8).
- [32] R.R. Yager and R.R. Yager, “On a general class of fuzzy connectives,” *Fuzzy Sets Syst.*, vol. 4, no. 3, pp. 235–242, 1980, doi: [10.1016/0165-0114\(80\)90013-5](https://doi.org/10.1016/0165-0114(80)90013-5).
- [33] M. Enea and T. Piazza, “Project selection by constrained fuzzy AHP,” *Fuzzy Optim. Decis. Mak.*, vol. 3, no. 1, pp. 39–62, 2004, doi: [10.1023/B:FODM.0000013071.63614.3d](https://doi.org/10.1023/B:FODM.0000013071.63614.3d).
- [34] J. Caha and A. Drážná, “Information about FuzzyAHP Package for R (ver.0.9.5)”. 2019. [Online]. Available: <https://cran.r-project.org/web/packages/FuzzyAHP/FuzzyAHP.pdf> (Accessed: Jul. 22, 2022).
- [35] M. Topolnicki, “Underpinning and lifting of civil engineering structures using controlled grouting processes – Podchwytywanie i podnoszenie obiektów budowlanych za pomocą kontrolowanych iniekcji geotechnicznych,” *XXV Konferencja Naukowo-Techniczna “Awary Budowlane”*, Międzyzdroje, Poland, vol. 24, no. 27.5, pp. 175–200, 2011 (in Polish).
- [36] M. Gwóźdź-Lasoń, “Numerical models of the subsoil reinforced by different kind of methods and technology,” PhD Thesis, Politechnika Krakowska im. Tadeusza Kościuszki, Kraków, 2007. [Online]. Available: [https://www.academia.edu/download/49792936/2007\\_GwozdzyLasonM\\_ModeleObliczeniowe.pdf](https://www.academia.edu/download/49792936/2007_GwozdzyLasonM_ModeleObliczeniowe.pdf) (Accessed: Apr. 22, 2023). (in Polish)
- [37] E. Falk, “Bodenverbesserung durch Feststoffeinpressung mittels hydraulischer Energie. Doctoral dissertation,” Technischen Universität Wien, Vienna, 1998.
- [38] A. Poteraj-Oleksiak, “Poziomowanie i stabilizacja gruntów – zalety metody iniekcji geopolimerowych,” *Mag. Autostrady*, no. 11–12, pp. 46–49, 2018.
- [39] A. Poteraj-Oleksiak, “Szybka technologia napraw oraz podnoszenia parametrów wytrzymałości konstrukcji nawierzchni drogowych przy pomocy iniekcji geopolimerowych,” *Drogoznictwo*, no. 6, pp. 171–177, 2019.
- [40] PN-B 03264:2002., *Konstrukcje betonowe, żelbetowe i sprężone. Obliczenia statycznie i wymiarowanie*, 2002.
- [41] W. Buczkowski, A. Szymczak-Graczyk, and Z. Walczak, “Experimental validation of numerical static calculations for a monolithic rectangular tank with walls of trapezoidal cross-section,” *Bull. Pol. Acad. Sci. Tech. Sci.*, vol. 65, no. 6, pp. 799–804, 2017, doi: [10.1515/bpasts-2017-0088](https://doi.org/10.1515/bpasts-2017-0088).